

PMu2e/LNF 2025

S. Bini, C. Bloise, V. Ciccarella (Dottoranda), F. Colao (Associato), G. Delle Monache,
E. Diociaiuti (Art. 36), S. Giovannella, P. Girotti (Assegnista), D. Hampai,
F. Happacher, M. Martini (Associato), S. Miscetti, L. Montalto (Associato),
D. Rinaldi (Associato), S. Salamino (Laureanda), I. Sarra (Responsabile Locale)

in collaboration with “LNF-SEA”: S. Ceravolo (Tecnico), M. Gatta (Tecnico)
the Detectors Development and Construction unit: A. Russo (Tecnico), D. Pierluigi (Tecnico)
and the Experimental Activities Support unit: B. Ponzio (Tecnico), E. Capitolo (Tecnico).

The assembly and commissioning of the Mu2e calorimeter has been successfully completed in the assembly clean room at SiDet, Fermilab. The calorimeter has been transported to the Mu2e hall and integration with the rest of the experiment is currently on-going. This report summarizes the commissioning and integration activities performed over the last year.

A full commissioning run in May 2025 successfully collected data from all 136 DIRAC boards, operating half of a calorimeter disk at a time, representing a crucial milestone for the Mu2e calorimeter. The data acquisition capacity was only limited by the power supply and DAQ servers availability at SiDet. The commissioning campaign achieved full characterization of the calorimeter system, including channel mapping, noise determination, time synchronization, and energy calibration. Over the second half of the year, the transport of both disks to the Mu2e experimental hall has been prepared and carefully conducted. The calorimeter now sits on the detector rails, together with the tracker and the muon beam stop. The complete integrity of the crystals, electronics, and optic fibers has been verified in place, confirming the success of the transport operations. While the installation of services from/to the TDAQ room is being completed, a temporary DAQ station has been prepared to collect data from one crate (160 channels) at a time, enabling DAQ integration activities. On the software side, full reconstruction routines are being developed and tested, including an online data quality monitor (DQM), the trigger reconstruction stream, and database entries of calibration constants.

1 Calorimeter assembly at SiDet

The Mu2e electromagnetic calorimeter [1, 2] consists of two annular disks, each containing 674 undoped Cesium Iodide (CsI) crystals with dimensions of $34 \times 34 \times 200$ mm³. Each crystal is read out by a dedicated Readout Unit (ROU), consisting of two custom UV-extended SiPMs and Front-End Electronics (FEE), housed within a protective copper Faraday cage. The FEE units are responsible for the amplification and shaping of the SiPM signals, providing pulses with a 150 ns width and 40 ns rise time. The readout structure is organized into 34 quasi-azimuthal sectors per disk with 20 crystals each, a configuration that averages irradiation effects over the radial distance from the beam center [3]. The electronic chain is based on two main components, the Mezzanine Boards (MZB) and the DIRAC digitization boards. The MZBs are responsible for the high-voltage distribution and the SiPM/FEE configuration via SPI, while regulating power using LTM8033 converters. The digitization of the 2696 analog signals is performed by 140 DIRAC boards across 10 crates per disk, using 12-bit ADCs sampling at 200 Msps [4]. An onboard MicroSemi SmartFusion2 FPGA performs online operations such as zero suppression, baseline calculation, amplitude extraction and time-stamping. Data transmission to the event builder is managed via dual-fiber optical links, while the MZBs are interfaced with the Detector Control

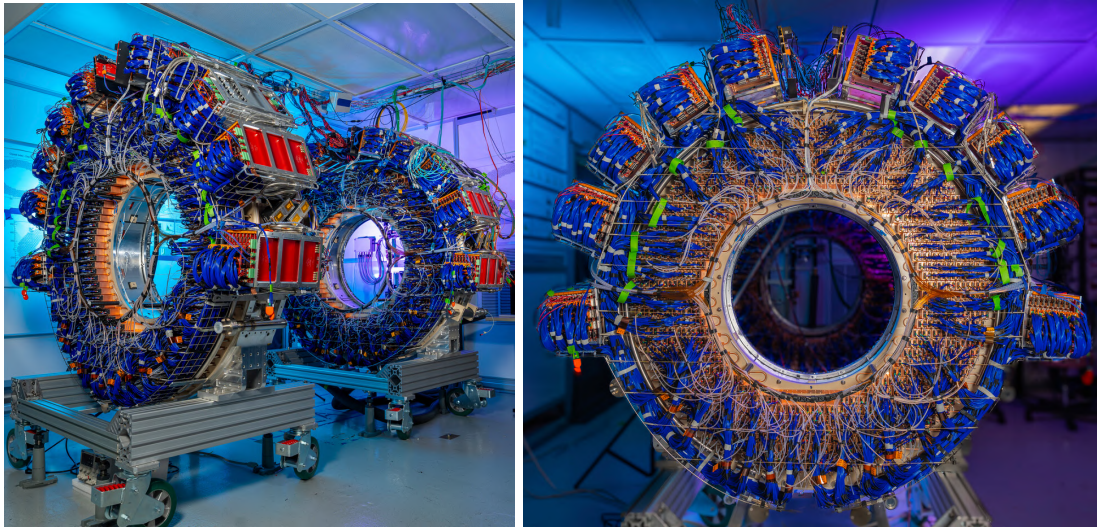


Figure 1: Calorimeter disks fully assembled at SiDet before transportation to the Mu2e hall.

System (DCS) via I2C.

The assembly process, carried out at Fermilab’s SiDet LabA cleanroom since late 2021, involved the crystal stacking on the aluminium support disks, the mechanical assembly of PEEK plates and custom crates and installation of separate cooling circuits for SiPMs and digital electronics. Following the ROU insertion and the integration of digital boards with copper cooling plates, activities in early 2025 focused on the final integration of the digital electronics and cable routing. The installation of all DIRAC boards was completed in March, followed by the routing of the FEE-MZB cables, the insertion of the breakout fibers, and the completion of the laser distribution system. Final steps included the installation of the temperature and radiation (TRAD) sensors on the front plate, as well as heaters and PT100 temperature monitors on the Inner Ring. Calorimeter disks fully assembled are shown in Figure 1.

2 Commissioning at SiDet

The commissioning of the calorimeter’s full readout chain in the assembly room at SiDet started in November 2024 with the downstream disk (Disk 1) and was completed in June 2025, with physics and calibration data successfully collected from all DIRAC boards. Cosmic rays and laser runs were acquired half-disk at a time to validate the detector functionality and to perform a first calibration and performance evaluation of the calorimeter.

2.1 Cosmic ray runs

During the commissioning run at the end of May 2025, roughly 16 hours of cosmic ray events were acquired, corresponding to $\sim 400\text{k}$ events for each half-disk. Figure 2 top-left shows an example of a cosmic ray event display. The energy deposition of Minimum Ionizing Particles (MIPs) measured by each readout channel was fitted to a Landau-Gaussian distribution to extract the Most Probable Value (MPV). The average response was around 550 (510) ADC counts/MIP for Disk-0 (Disk-1), corresponding to 27 (25) ADC/MeV, with a spread $\sigma/\mu \sim 9\%$ for both disks. After energy

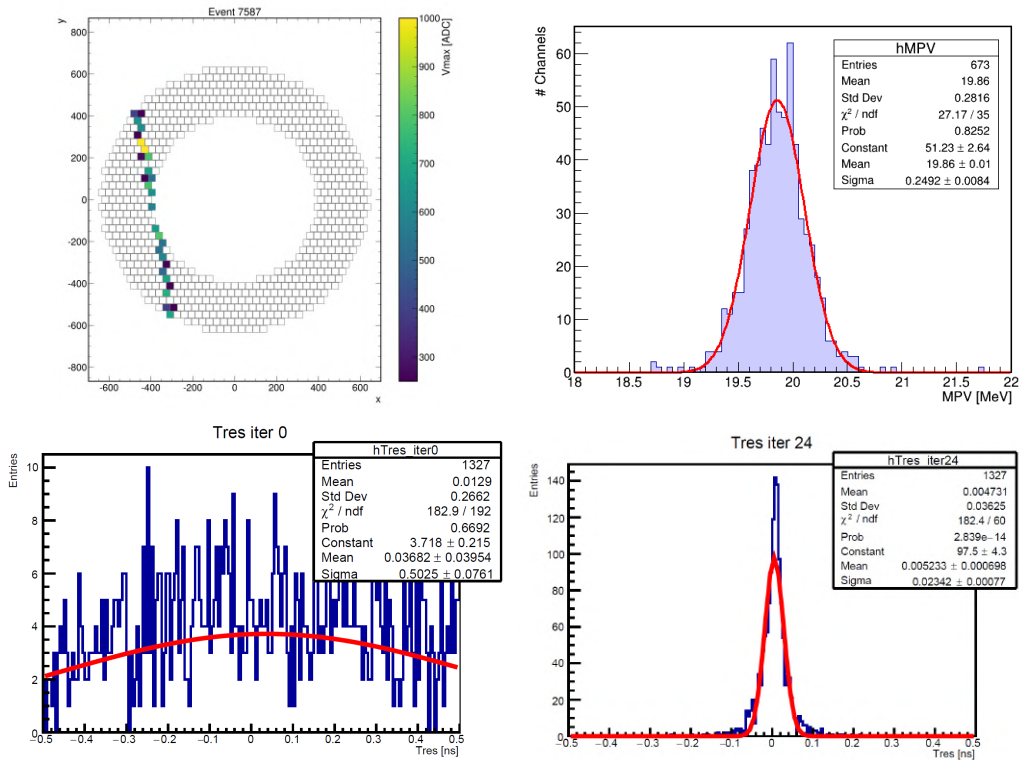


Figure 2: Top-left: example of a cosmic ray track in the calorimeter during SiDet data taking. Top-right: distribution of the MPV of the MIP energy deposition for half of the Disk 1 channels after energy scale calibration. Bottom: distribution of the time residuals at the first (left) and last (right) iteration.

calibration, the relative spread of the reconstructed peak of the MIP energy depositions showed channel-to-channel variations within 1.2% (Fig.2 top-right). In parallel, hardware adjustment of the SiPMs' bias voltage was performed to equalize their response to 19 ADC counts/MeV, resulting in a reduction of the channel-by-channel spread to 3.8%.

The time calibration of all readout channels was performed through a two-step procedure based on MIPs. An initial algorithm was developed to align the relative time offsets between the two SiPMs of each crystal using their measured time difference and mean time. This was followed by an iterative procedure that aligns all channels by minimizing the time residuals from cosmic ray tracks. The algorithm was optimized and tested on SiDet data, providing a reduction of the initial residuals spread from ~ 500 ps (Fig.2-bottom left) to less than 25 ps (Fig.2-bottom right) with 25 iterations.

2.2 Laser runs

The pulsed laser system was employed to uniformly illuminate the crystals, allowing for studies of the consistency between the two readout channels of each crystal. Asymmetry studies between the left and right SiPMs of the crystals demonstrated excellent energy resolution after energy calibration, ranging from 1.5% to 3% (Fig.3-left). Furthermore, a dedicated intensity scan was

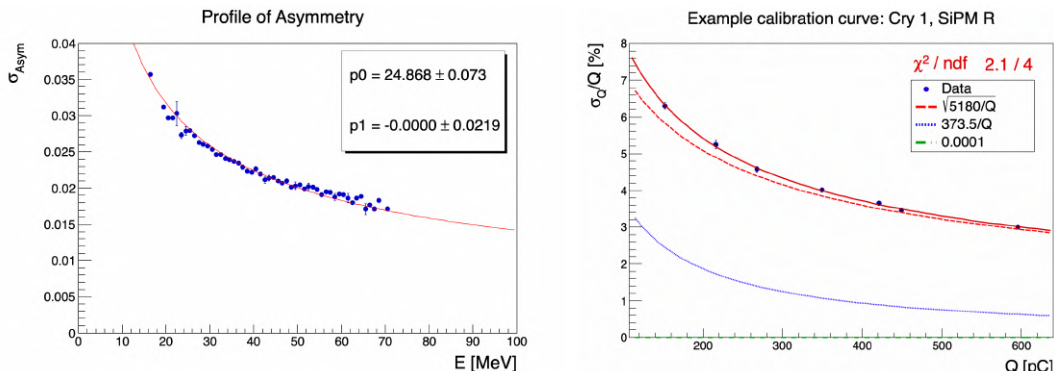


Figure 3: Left: asymmetry profile as a function of energy for all channels of the upstream disk (Disk 0). Right: example of calibration curve for a single ROU.

performed by varying the laser attenuation with a filter wheel to evaluate the gain of each SiPM. The photosensors gain was extracted from the charge calibration curves (Fig.3-right), yielding an average of 3.7×10^6 , in excellent agreement with the quality control measurements previously performed at LNF.

2.3 Calorimeter performance

The calorimeter’s performance was characterized using both cosmic rays and laser data. The energy resolution for cosmic ray events exhibited a behavior consistent with its expected parametrization, reaching 6% at 100 MeV and with a constant term of 2.5%. These results were compared with a Monte Carlo simulation of the full experiment and found to be in good agreement, as shown in Figure 4 top-left. The complementary study of the asymmetry with the laser allowed to extract a mean light yield of crystals of 22 photoelectrons per MeV, in agreement with construction parameters (Figure 4 bottom-left).

The time resolution as a function of energy was also evaluated with MIP and laser events. Results are reported in Figure 4-right. The laser data showed a purely stochastic behavior and a constant term below 40 ps. For cosmic ray data, the timing response was found to be in good agreement with Monte Carlo simulated events, with a stochastic term consistent with the results obtained from the laser analysis.

3 Calorimeter transport to the experimental hall

Extensive work has been carried out to perform the delicate transportation of the calorimeter disks to the Mu2e experimental hall. This activity, consisting both of a critical lift and transportation, was carried out under responsibility of the Mu2e team of LNF. The transport was completed successfully in September 2025.

The total weight of each calorimeter disk corresponds to around 1450 kg. A dedicated transport tool was designed, fabricated, and tested with dummy weights in May 2025. The transport tool is composed of two pieces: a Lifting Fixture and a Transport Stand. The Lifting Fixture is a "C" shaped main frame bolted to the calorimeter’s monolithic aluminum outer ring at three attachment points: two at the bottom for weight support and one at the top for vertical stabi-

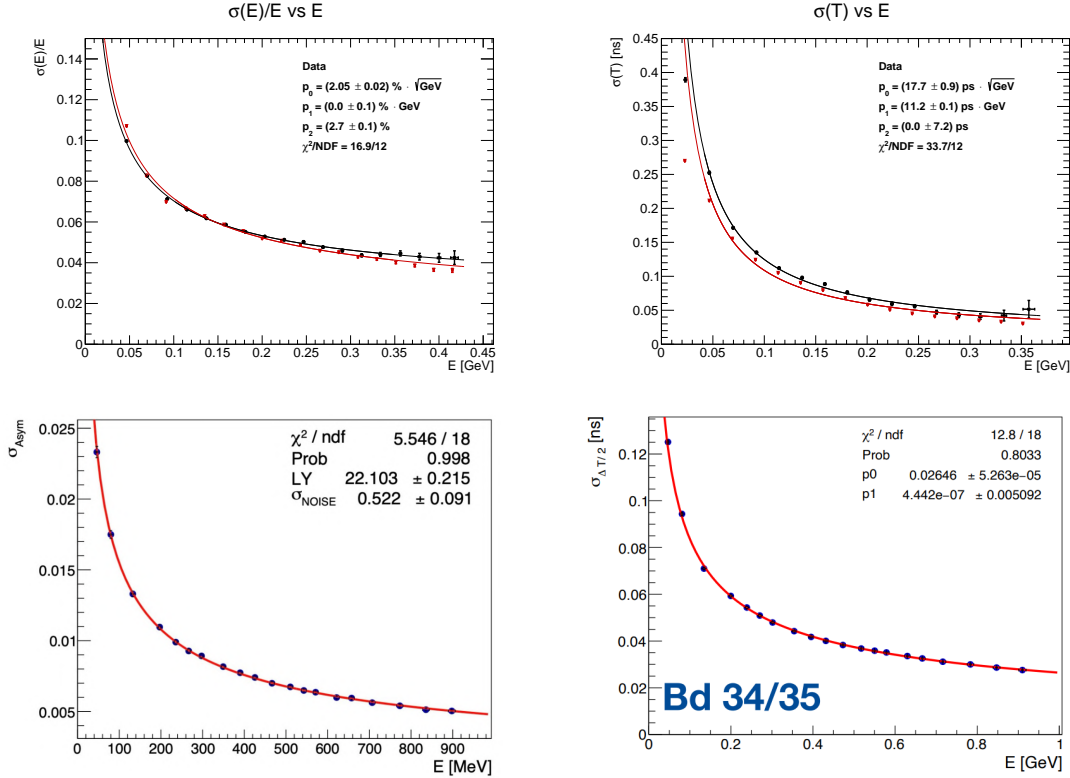


Figure 4: Energy (left) and time (right) resolution as a function of energy with cosmic rays (top) and laser (bottom) events.

lization. The lifting cranes are connected to the lifting fixture through a CoG X-Z adjustment mechanism that allows for a perfect balance of the load at all times. The Transport Stand is a base that allows to rest the Lifting Fixture together with the calorimeter for transportation. It is equipped with a damping system to simultaneously ensure a tight connection to the truck and to suppress vibrations during the drive from the assembly lab to the experimental hall.

The downstream disk was transported to the Mu2e experimental hall building on September 11th, 2025, while the upstream disk was transported on September 16th, 2025. Figure 5 shows the transport phases of Disk 1.

4 Calorimeter installation and services

After the calorimeter was installed on the rails, work began to install the calorimeter feed-through flanges on the IFB. The two flanges have been leak-tested with the vacuum chamber at SiDet lab, and then mounted on the IFB in November, 2025. Cable trays have been installed over the muon beam stop (MBS) and on the calorimeter (Figures 6, 7). Vacuum side TDAQ fibers, LV/HV lines, and laser fibers have been layed on the trays and connected to the calorimeter on one end and to the flanges on the other end. A cable slack between the calorimeter trays and the MBS ones allows for limited but independent movement of the two pieces on the rails. On the external side, power connectors have been installed and routed toward the terminal blocks on the support mesh

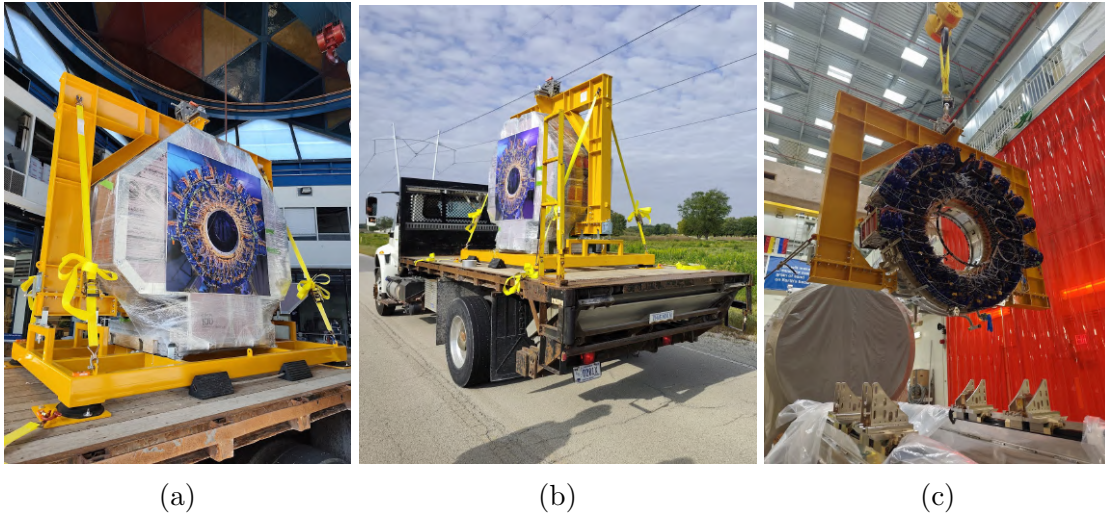


Figure 5: Transport of a calorimeter disk from SiDet to the Mu2e hall. The disk is loaded onto the truck (a), transported to MC-2 (b), and lowered onto the experiment rails (c).

(Figure 8). Temporary safety ground lines have been connected to the calorimeter disk and to the terminal blocks in order to operate the electronics before completing the cabling. Work is now in progress to attach the cable trench saddle to the IFB and to finish the connection of all cables and fibers. In the DAQ room, all the power cables and TDAQ fibers have been connected to the power supplies and TDAQ servers. The laser table has been assembled in the same room and the laser optics aligned to service the twelve calorimeter fibers.

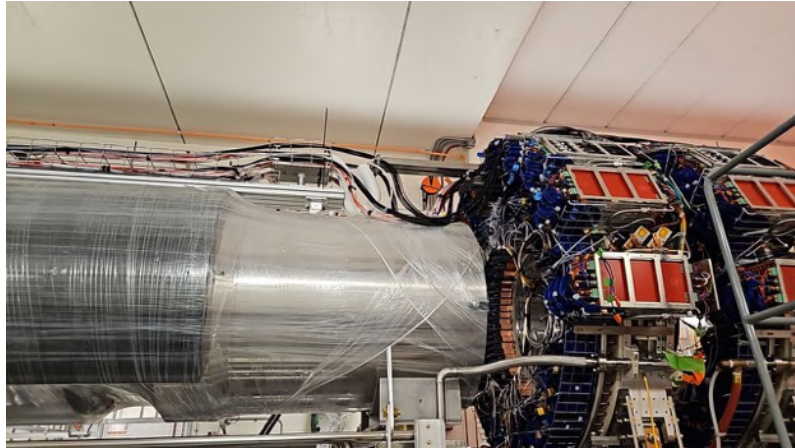


Figure 6: Cable trays over the muon beam stop. The cable slack between the calorimeter and the muon beam stop allows for independent movement of the calorimeter on the rails.

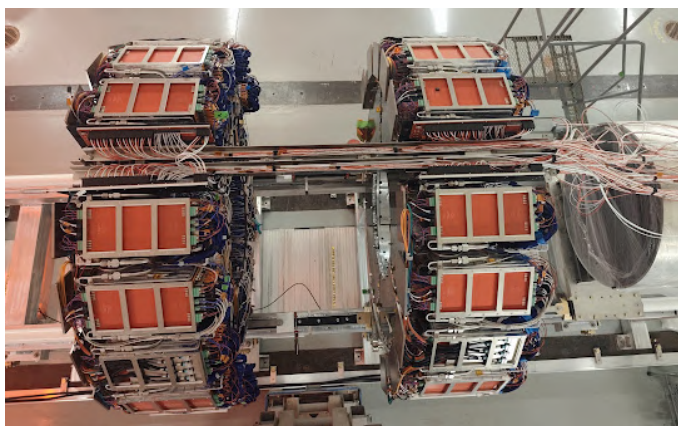


Figure 7: Cable trays over the calorimeter.

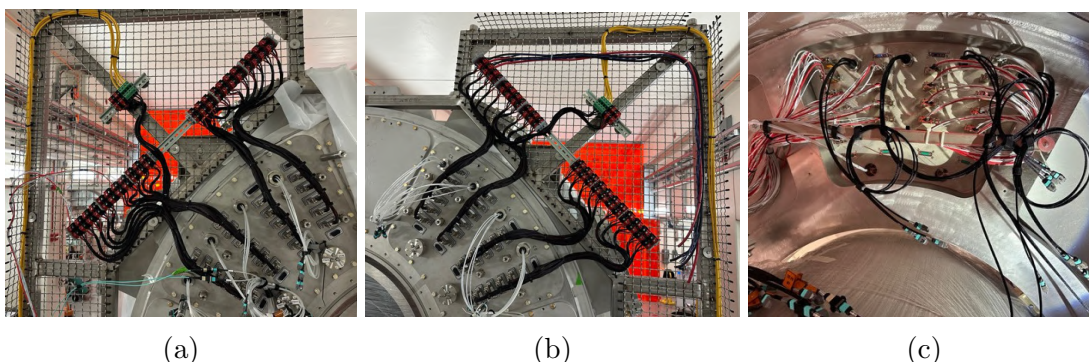


Figure 8: (a, b) The feedthrough flanges installed on the IFB, with power connectors installed and routed toward the terminal blocks. (c) Vacuum-side of the left flange.

5 Commissioning in the hall

A few hours after the disks were positioned on the rails, a quick test of all calorimeter channels was performed to check for any possible damage during transportation. Since the chiller system was not yet installed and to avoid overheating, the quantity of channels readout and the readout time were minimized. The test was carried out by powering one crate at a time, collecting events for only 100 seconds (10^6 triggers). Slow control readings from each DIRAC and MZB board, together with noise and cosmic runs, confirmed that all calorimeter channels were still operational and functioning properly.

In order to resume larger-scale commissioning work at the experimental hall while full service integration was underway, a temporary servicing station was assembled to provide voltage to one crate. Two TDAQ fibers extensions have been used to connect one IFB feedthrough flange to the fibers in the trench. One chiller station has been connected to a local server for control and software interlock. This allowed to resume the calorimeter DAQ development and begin integration with the rest of the experiment DAQ.

6 Reconstruction software

To support the commissioning activities, work has been done to develop the software needed to decode, calibrate, and reconstruct the calorimeter signals. Raw data decoders interpret the digitized output coming from the DIRAC boards for all running modes. Fast decoding variants have been developed to sustain the online trigger rates. An online data quality monitor (DQM) stream has been developed for fast diagnostic of the detector performance. Offline database infrastructure and calibration tables have been implemented into the reconstruction workflow. Online database tables have been implemented to configure the calorimeter electronics and perform online trigger reconstruction. Calorimeter reconstruction output has been added to the experiment-wise ROOT analysis n-tuples. Finally, a ROOT-based calorimeter disk histogramming tool has been developed to visualize calorimeter hits and quantities.

7 Theses

- S. Salamino, “Energy and Time Performance of the Mu2e Electromagnetic Calorimeter”, master thesis at the Università degli Studi La Sapienza.

8 List of Conference Talks/Posters by LNF Authors in the Year 2025

- S. Miscetti, Status and perspectives of Mu2e experiment, Muon4Future 2025, Venezia, IT.
- S. Miscetti, Searching for CLFV with muon to e conversion: Mu2e and COMET status, FCCP 2025, Anacapri, IT.

9 Publications

- S. Miscetti, and the Mu2e Collaboration, “Status of the Mu2e experiment”, Nucl.Instrum.Meth.A 1073 (2025) 170257, DOI: <https://www.doi.org/10.1016/j.nima.2025.170257>
- L. Borrel *et al.*, “The Mu2e Calorimeter”, PoS ICHEP2024 (2025) 1060, DOI: <https://www.doi.org/10.22323/1.476.1060>
- N. Atanov *et al.*, “Development, production, and testing of the Mu2e Calorimeter Silicon Photomultipliers”, JINST 20 (2025) 08, P08004, DOI: <https://www.doi.org/10.1088/1748-0221/20/08/P08004>
- N. Atanov *et al.*, “Status of the Mu2e calorimeter readout electronics”, <https://www.osti.gov/biblio/2562841>, submitted to Nucl.Instrum.Meth.A
- N. Atanov *et al.*, “Crystal Calorimetry for Charged Lepton Flavor Violation Searches”, PoS WIFAI2024 (2025) 030, DOI: <https://www.doi.org/10.22323/1.489.0030>

References

1. N. Atanov *et al.*, “The Calorimeter Final Technical Design Report”, arXiv:1802.06341 (2018).
2. N. Atanov *et al.*, “The Mu2e Crystal Calorimeter: An Overview”, Instruments 2022, 6(4), 60.
3. S. Giovannella *et al.*, “Updates on calorimeter dose estimate”, Mu2e-doc-23833, January 2019
4. N. Atanov *et al.*, “Mu2e Crystal Calorimeter Readout Electronics: Design and Characterisation”, Instruments 2022, 6(4), 68.